iConclusions https://iconclusions.com/ Conclusions in Engineering

A Theoretical Study for Investigation of Structural, Optical, Electronic, and Mechanical Properties of Double Perovskites Halide for Solar Cell Application

Ali Yaqoob,[1] **Nawishta Jabeen**,[2, a)] **Imtiaz Ahmad Khan**,[1] **Ameer Hamza**,[1] **Irfan Haider**,[1] **Fatima Kainat**,[1] and **Ahmad Hussain**[1, b)]

[1)] *Department of Physics, The University of Lahore, Sargodha campus, 40100 Sargodha, Pakistan*

[2)] *Department of Physics, Fatima Jinnah Women University, 46000 Rawalpindi, Pakistan*

ABSTRACT: For the calculation of structural, optical, electronic and mechanical properties of a X_2ScTlI_6 with $X = Cs, Li, Na$ and K possessing a cubic (2 25) structure a density functional theory (DFT) approach has been employed. The Perdew-Burke-Ernzerhof (PBE) approach and alongside generalized gradient approximation (GGA) are employed to investigate the structural, bandgap topologies, density of states and optical parameters of the compounds. High values of optical parameters like absorption $(\alpha = 10^5\ cm^{-1}$) with direct band gap in semiconductor range of (2.05 eV to 2.42 eV) along with enhanced dielectric functions, refractive index, reflectivity, extinction coefficient, in the spectra of visible and ultraviolet region is observed and total and partial densities of states are also investigated for application in optoelectronic devices such as solar cells. The Pugh's ratio indicates these materials exhibit a nature that is also beneficial for solar cells, especially in applications requiring flexibility and mechanical durability..

Received: 17 December 2024
Accepted: 03 March 2025
DOI: https://doi.org/10.71107/8z89j617

I. INTRODUCTION

The usage of diverse conventional energy sources which includes burning of fossil fuels, coal, natural gas, petroleum, agriculture stalk and others for so many years had caused hazard to environment including water and air pollution, global warming, acid rain and soil eruption which led to serious life sustainability problems. So only solution to this exist as if we move from usage of such conventional fuels to renewable energy sources which include wind and hydro power, solar energy, and other sources. One of the most important sources of energy is sun. The sun radiates more energy in one second than people have used since beginning of time[1]. The problem with Solar energy is that it cannot be used directly, we require some device which can convert solar energy into other useable form of energy. One significant strategy for converting energy is to develop photocatalytic (PC) or photovoltaic (PV) technologies, like solar cells (SC) which we use to transform sunlight into chemical, electrical and other useful form of energies[2,3].

Semiconductor materials with an appropriate bandgap to absorb light from sun for production of free electrons. The scientific community have established some of the solar cells and classified them in different families on the basis of different materials used like, perovskite solar cells [4] thin-film amorphous silicon solar cells,[5] gallium copper indium selenide solar cells,[6] cadmium telluride solar cells,[7] organic solar cells,[8] etc. in this race of developing more and more efficient solar cells, scientists are working on these discussed families. One of the most important of them are the perovskites solar cells whose production required little effort and less expenditures.

Recently, researches have been made on the double perovskites materials which originates from simple ABO_3 type perovskites with general formulae,

[a)] Electronic mail: nawishta.jabeen@fjwu.edu.pk
[b)] Electronic mail: ahmed_00277@yahoo.com

$AA'BB'X_6$, (where A or A′ belongs to the group I and group II of periodic tables on the other hand transition metals are placed at B or B' and X represents halogen (like F, Cl, Br, I).

Jong et al. performed the theoretical calculations of structural ,optical and electronic properties of (K_2SnBr_6) and monoclinic (K_2SnI_6) compounds with cubic symmetry for the production of doublewalled, high-efficiency perovskite with low cost has successfully predicted their application as solar cell[9]. Mahmood et al. have performed the ab initio study of double perovskites originate from general formula like Rb_2PtCl_6 and Rb_2PtBr_6 occupy the energy band gap valued 2.6 eV and 2.1 eV respectively. Also, showing maximum optical conductivity in visible region existing in 1.61 eV to 3.19 eV energy spectra. These properties indicating potential usage of these materials for SC with huge stability and up-to high conversion efficiency[10].

Albalawi performed study on materials $Cs_2KTlX_6(X = Br, Cl, I)$ for their optical, electronic and transport properties by using density functional theory which also indicates semiconducting nature of these materials due to presence of halogen and Tl atoms. This study predicted that the existence of halogen group and transition metal Tl mainly contributed to the valance and conduction band edges[11].

Ahmad et al. performed DFT-based research by using WIEN2k and BoltzTraP programs, shows the structural, elastic, optoelectronic, and transport properties of a double perovskite $Na_2CuMXX_6(M = Sb,\ Bi; X = Cl, Br)$. Its potential uses in solar cells were also suggested by the materials' indirect bandgap and encouraging optical absorption in range of $(1.7 - 3.4eV)$[12].

Another study performed by S. Mahmud by using DFT to examine the phase stability, optoelectronic, and thermoelectric characteristics of $X_2AuYZ_6(X = Cs, Rb; Z = Cl, Br, I)$ double perovskites. Mechanical and thermodynamic stability were predicted by Pugh's ratio, phonon dispersion, and formation energy, whereas tolerance and octahedral factors were used to prove structural stability. The materials also show promise for solar and thermoelectric applications because of their visible-to-UV band gaps, which range from 1.74 to 2.91 eV[13]. The structural, optical, electronic and mechanical properties of X_2ScTlI_6 ($X = Cs, Li, Na, K$) in a cubic (225) phase remain unexplored, particularly for their potential in optoelectronic applications. This study employs density functional theory (DFT) using the PBE-GGA approach to analyze the structural, electronic, and optical properties of X_2ScTli_6 compounds aiming to assess their potential for optoelectronic applications, particularly in flexible and durable solar cells.

In our presented work we have established a theoretical framework for studying the elastic, structural, alongside optoelectronic properties of the X_2ScTlI_6 where ($X = Cs, Li, Na$ and K) to investigate their potential usage in photovoltaic technology like Solar cells.

II. MATERIALS AND METHODS

First-principle calculations were carried out on Cambridge Serial Total Energy Package (CASTEP)[14] which used plane-wave pseudopotentials and Perdew-Burke-Ernzerhof (PBE)[15] as exchangecorrelation functional along with generalized gradient approximation (GGA)[16] of density functional theory (DFT) using material studio. GGA-PBE approach was used to calculate the electronic structure of these perovskites because it offers an excellent mix between computational efficiency and accuracy. GGA-PBE is a good fit for our work because it has been demonstrated in earlier research on related structures[17,18] to precisely characterize their band gaps, optical and electrical characteristics.

Unit cell atomic positions and lattice parameters of all the structures were optimized within this code. Broyden- Fletcher-Goldfarb-Shanno (BFGS)[19] algorithm technique was utilized for this optimization, by keeping the value of self-consistent field (SCF) to be 1.0×10^{-6}Å, total energy was fixed to 2.0×10^{-5}eV/ atom, maximum stress and maximum force was of 0.1 GPa , and 0.05eV/Å, valued respectively, and taking 0.002Å as maximum displacement. Structural parameters, electronic and optical properties were carried out by using 450 eV as plane-wave cut-off energy alongside the k integration of Monkhorst pack grid[20] as $5 \times 5 \times 5$ k-point mesh throughout the Brillouin zone. Furthermore, van-der-walls interactions were considered by using the TS method of correction. For calculation of the band-structure CASTEP uses set of quantum mechanical equation[21] given as

$$\psi_{ki}(r) = \exp[ik \cdot r] f_i(r) \tag{1}$$

$$f_i(r) = \sum_G G_{i,G} \exp[iG.r] \tag{2}$$

$$\sum_{G'}\left[\frac{h^2}{2m}|k+G|^2\delta_{GG'}+V_{ion}\left(G-G'\right)+V_H\left(G-G'\right)\right]C_{i,k+G'}=\varepsilon_i C_{i,k+G} \tag{3}$$

Here φ represents the pseudo wave function, k is wave vector, and r shows the radial distance in spherical coordinate for a point given in space. G is unique constant density function, V_{xc} is exchangecorrelation potential, V_{ion} is ionic potential δ_{GG} represents the Kronecker delta function which are important parameters in calculating the electronic properties.

Optical properties (including both the real and imaginary portion of dielectric function and refractive indices, reflectivity, optical conductivity, absorption, and loss function) were calculated directly and indirectly by Kramers-Kronig dispersion relations[22]. The complex of dielectric function is described as

$$\varepsilon(\omega)=\varepsilon_1(\omega)+i\varepsilon_2(\omega) \tag{4}$$

$$\varepsilon_1(\omega)=1+\frac{2}{\pi}P\int_0^{\infty}\frac{\omega'\varepsilon_2(\omega')}{\omega'^2-\omega^2}d\omega' \tag{5}$$

$$\varepsilon_2(\omega)=\frac{4\pi^2e^2}{m^2\omega^2V}\sum\int_{BZ}|\langle\psi_k^v|\,\overrightarrow{pl}\,|\psi_k^C\rangle|^2\,\delta\left(E_{\psi_k^c}-E_{\psi_k^v}-\hbar\omega\right) \tag{6}$$

Electronic occupied and unoccupied states can be expressed as the momentum matrix which is the story behind the imaginary portion of dielectric function and can be directly obtained by using Kramers-Kronig dispersion relations whereas, the real portion of the dielectric function dependent on incident light frequency can be obtained from this imaginary part. For the calculation of imaginary portion of dielectric function some terms like ψ_k^c is the conduction band wave function and valance band wave function are denoted by ψ_k^v at k wave function, e is the electronic charge, V is volume of unit cell, and ω is frequency of photon, given in (6). Remaining optical properties were obtained indirectly[23,24] from Kramers-Kronig dispersion relations by using the following expressions.

$$n(\omega)=\left\{\frac{\sqrt{\varepsilon_1^2(\omega)+\varepsilon_2^2}(\omega)}{2}+\frac{\varepsilon_1(\omega)}{2}\right\}^{\frac{1}{2}} \tag{7}$$

$$k(\omega)=\left\{\frac{\sqrt{\varepsilon_1^2(\omega)+\varepsilon_2^2}(\omega)}{2}-\frac{\varepsilon_1(\omega)}{2}\right\}^{\frac{1}{2}} \tag{8}$$

$$R(\omega)=\frac{(1-n)^2+k^2}{(1+n)^2+k^2} \tag{9}$$

$$\alpha(\omega)=2\omega\left(\frac{\left[\sqrt{\varepsilon_1^2(\omega)+\varepsilon_2^2(\omega)}-\varepsilon_1(\omega)\right]}{2}\right)^{\frac{1}{2}} \tag{10}$$

$$L(\omega)=\frac{\varepsilon_2(\omega)}{\varepsilon_1^2(\omega)+\varepsilon_2^2(\omega)} \tag{11}$$

Mechanical parameters including elastic stiffness constants were obtained by using module 'Forcite' within material studio which uses charges as 'assigned' under 'universal force field', and at 'ultra-fine' quality. 'Ewald' was used as the electrostatic summation method and 'atom-based' summation was chosen as for 'Van der Waals'. From these calculated values of elastic constants, the value of different modulus like Bulk (B), shear (G) and young's modulus (Y) and value of Poisson's ratio (v) were obtained by using following relations[25,26].

$$B_H=\frac{1}{2}\left(B_v+B_R\right) \tag{12}$$

$$G_H = \frac{1}{2}(G_v + G_R) \tag{13}$$

$$Y = \frac{9B_H G_H}{3B_H + G_H} \tag{14}$$

$$v = \frac{3B_H - 2G_H}{2(3B_H + G_H)} \tag{15}$$

III. RESULTS AND DISCUSSION

A. Structural Properties

X2ScTII 6 with X = Cs, Li, Na and K occupies cubic symmetry with space group Fm3m (225) represented in Fig. 1. There exists a total of 40 atoms in the unit cell structure, with 8 ' X' site atoms ($X = \mathrm{Cs, Li, Na}$ and K), 4$'$Sc ' atom and also 4$'$Tl$'$ atom and the remaining positions belongs to ' I ' atom alone. As it's a cubic structure so all the lattice parameters are same like $\mathbf{a} = \mathbf{b} = \mathbf{c} = 12.56$Å, and $\alpha = \beta = \gamma = 90°$.

B. Electronic Properties

The nature of the materials which classifies them as conductors, semiconductors, or insulators, can be determined on basis of their energy band gap. Overlapping of the valence band (VB) and the conduction band (CB) proposed the conducting nature while subtracting the conduction band (CB) minimum from valence band (VB) maximum predicts the insulator and semiconductor natures of the compounds. Calculated energy band structures of X_2ScTII6 with X = Cs, Li, Na and K , by using GGAPBE approximation are shown in Fig. 2 respectively. Our calculations show that Cs_2ScTlI, Li_2ScTlI6, Na_2ScTl_6 and K_2SCTll_6 are all direct band gap semiconducting compounds with value ranging 2.05 eV to 2.42 eV . A direct band gap showing strong effect of spin-orbit coupling near the G symmetry point and this is the point of band gap value.

Density of states confirms the presence of desired band gap across the fermi level 0 eV denoted by dotted vertical line shown in Fig. 3. Alongside partial density of states was also calculated to check each atomic orbital contribution in creating the band structure and are presented in Fig. 4.

Fig. 4a representing PDOS of Cs_2ScTlI_6, in which the majority contribution in establishing the valance band is due to presence of $\mathrm{I} - 5\mathrm{p}^5$, other to this we have very little contribution of $\mathrm{Tl} - 6\ \mathrm{s}^2$ and $\mathrm{Sc} - 4\ \mathrm{s}^2$ in formation of valance band. The highest energy gap is found in this compound compared to others, lie between 0 and 2.5 eV , On the other hand, in case of conduction band we got $\mathrm{Cs} - 4\ \mathrm{d}^{10}, \mathrm{Cs} - 5\mathrm{p}^6$ and $\mathrm{Sc} - 3\ \mathrm{d}^1$ showing maximum contribution. The Cs-6s $^1, \mathrm{Tl} - 6\mathrm{p}^1$ and $\mathrm{I} - 5\ \mathrm{s}^2$ shows negligible contribution to the conduction band of Cs 2 ScTlI .

Fig. 4b presents huge dominance by the I-5p ^{5} in the valance band area of Li2ScTlI6. Tl-6s ^{2} and $\mathrm{Sc} - 3\ \mathrm{d}^1$ demonstrate a weak impact, while I-5p ^{5} is very much prominent in here. Li2ScTlI6 possess an energy band gap of 2.05 eV , consistent with previously shown electronic band structure. The impact of I-5p ^{5} and $\mathrm{I} - 5\ \mathrm{s}^2$ is very weak in case of conduction band. In this region Li-1s $^2, \mathrm{Li} - 2\mathrm{p}^1$ and $\mathrm{Sc} - 3\ \mathrm{d}^1$ shows significant contribution.

From Fig. 4c we conclude that valance band mainly represents an outcome of hybridization of the $\mathrm{I}5p^5, \mathrm{Tl} - 6\ \mathrm{s}^2$, and $\mathrm{Sc} - 3\ \mathrm{d}^1$, states, but $\mathrm{Sc} - 3\ \mathrm{d}^1$ shows minute presence. The I atom showing significant influence over other atoms in the valance band. No electronic state of any type exists in the electronic band gap range of about 0 and 2.3 eV . Sc and Na showing influence in the conduction band of Na2ScTlI 6 . Specifically, the states $\mathrm{Sc} - 3\ \mathrm{d}^1, \mathrm{Na} - 2\mathrm{p}^6$ and $\mathrm{Na} - 3s^1$ exert noteworthy effects, whereas the $\mathrm{Tl} - 6\mathrm{p}^1$ state revels minimal appearance.

The PDOS for K_2ScTlI_6 can be seen in Fig. 4d, where I and Tl ions are overriding in the valance band, with Sc and K making negligible existence. Valance band of this compound is pointedly inclined by $\mathrm{I}5p^5, \mathrm{Tl} - 6\ \mathrm{s}^2$ states. This material's experience a bandgap between 0 and 2.4 eV which is forbidden energy region. In the conduction band $\mathrm{Sc} - 3\ \mathrm{d}^1$, $\mathrm{K} - 3\ \mathrm{s}^2$, $\mathrm{K} - 3\mathrm{p}^6$ and $\mathrm{K} - 4\mathrm{p}^1$ are the one with prominent contribution compared to others elements. The I-5 p ^{5} and I-5s ^{2} ions is showing negligible contribution to the CB.

C. Optical Properties

The complex dielectric function is described as given in equation 4. The graphs for complex dielectric functions (real and imaginary) are plotted in the energy range $0 - 9$eV in Fig. 5a and b, respectively. The $\varepsilon_1(0)$ values for $Cs2_2ScTlI_6, Li_2ScTlI_6, Na_2ScTlI_6$ and K_2ScTlI_6 are $4.68, 4.72, 4.62$ and 4.55 respectively which is the most important parameter in these spectra discussed at zero-frequency limit $\varepsilon_1(0)$, representing the electronic part of the dielectric function[27]. Peaks values of $\varepsilon_1(\omega)$ describing the maximum polarization lies in the visible region with peaqk value of 6.84 at 2.4 eV shown by the one with minimum band gap value 2.05 eV of Li_2ScTlI_6 materials. Peaks value of 6.75 for Cs_2ScTlI_6 is at 2.51eV, 6.72 for Na_2ScTlI_6 is at 2.44 eV , and 6.63 for K_2ScTlI_6 is

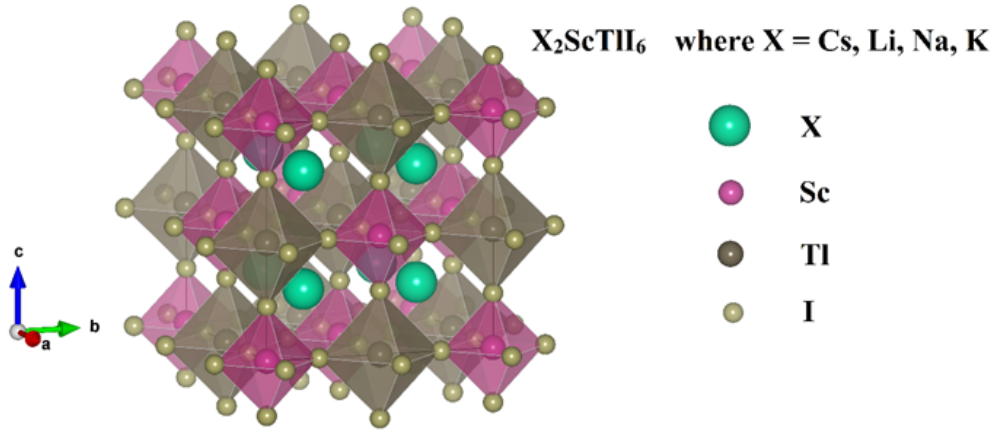

FIG. 1: Cubic structured of the materials X2ScT1I6 with (X = Cs, Li, Na and K).

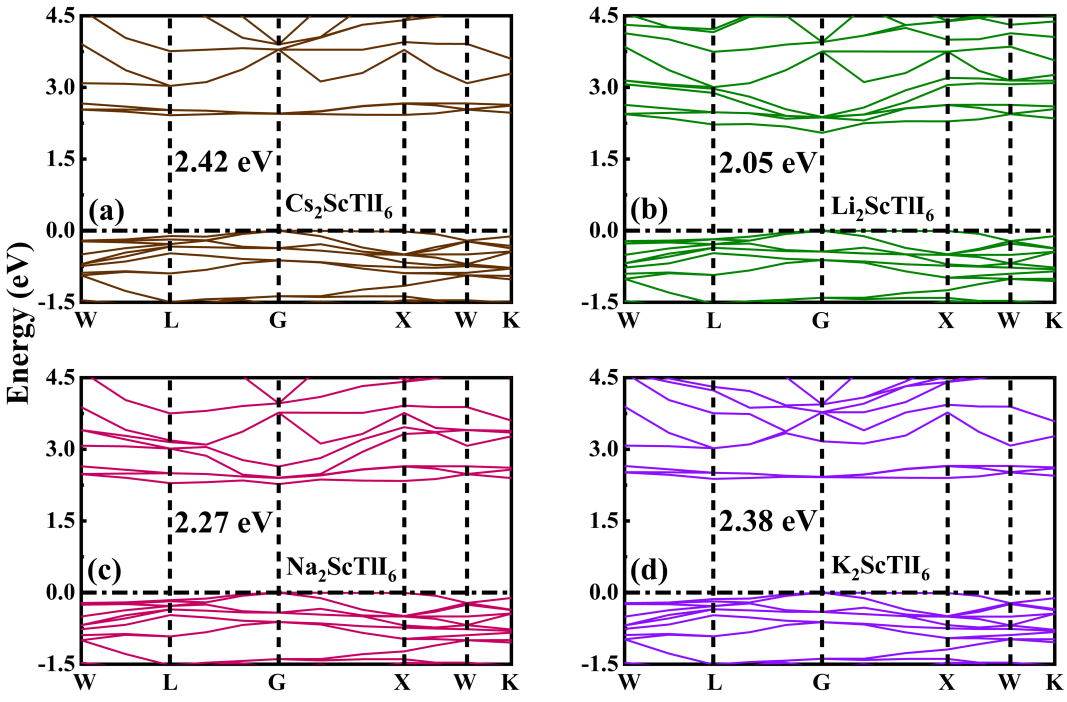

FIG. 2: Band Structure of the materials (a) Cs_2ScTlI_6, (b) Li_2ScTlI_6, (c) Na_2ScTlI_6, and (d).

at 2.5 eV .

Various inter-band transition within materials band structures is characterized by the peaks observed in the $\varepsilon_2(\omega)$ plots. From the plots in Fig. 5b, it is clear that for visible region, Li_2ScTlI_6 exhibits the highest peak value 4.9 at 3.2 eV , when compared with the other structures. This is because of the lower band gap for Li_2ScTll_6 compared to the other materials, which makes it easier for the polarized electrons to extend into the conduction band and enhance the photovoltaic effect. Cs2ScTlI 6 shows the lowest peak of about 4.4 at 3.3eV, Na_2ScTlI_6 shows peak at 3.2 eV of valued 4.8 and K_2ScTlI_6 shows

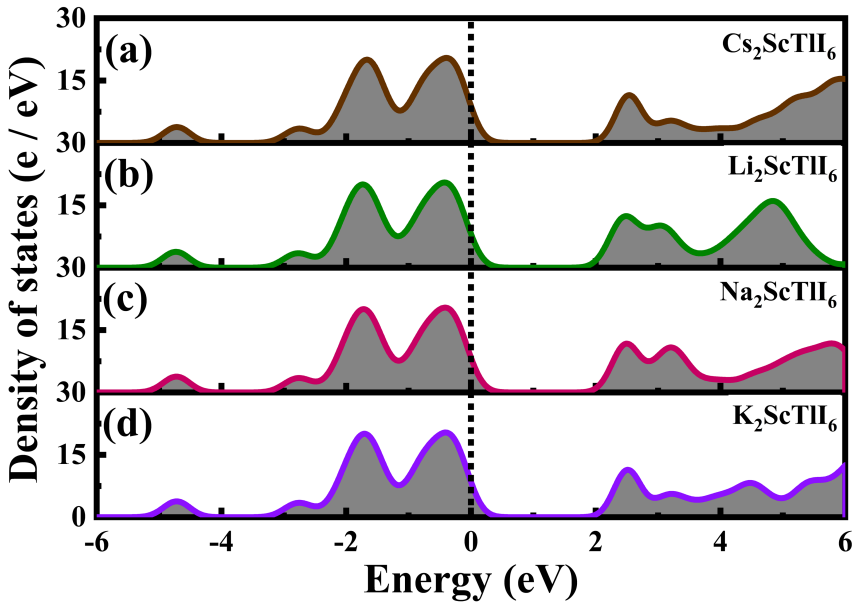

FIG. 3: Density of states of materials (a) Cs2ScTlI6, (b) Li2ScTII6, (c) Na2ScTII6, and (d) K2ScTII6.

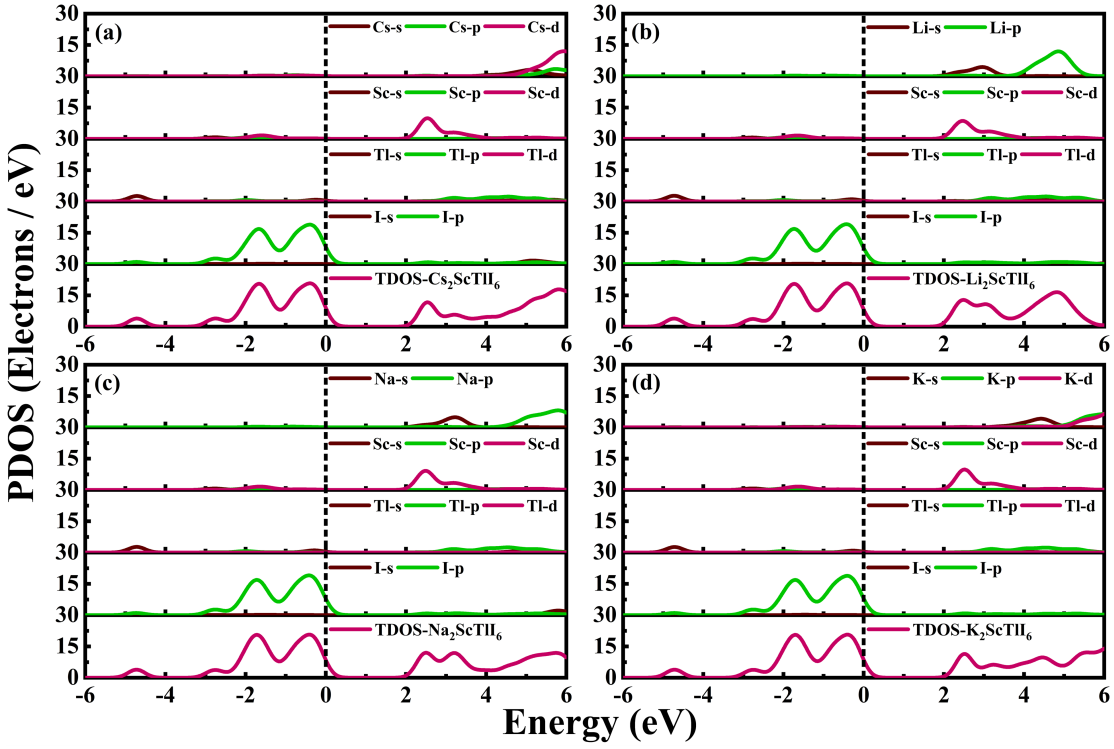

FIG. 4: Partial density of states of materials (a) Cs2ScTlI 6 , (b) Li2ScTlI 6 , (c) Na2ScTII6, and (d) K2ScTlI 6.

peak at 3.3 eV of valued 4.5.

Complex of refractive index can be described by the combination of refractive index and extinction coefficient shown in Fig. 5c, 5d. Refractive index shows similar behavior as comparison with the real of dielectric function. To be utilizing these materials for practical applications especially in opto-electronic devices, the refractive index $n(\omega)$ information plays a crucial role as in (7), indicating the data response to materials transparency; as $n(\omega) \geq 1$ entitles the optical substance as transparent nature. Threshold value of refractive index can be seen highest for Li_2ScTlI_6 of about 2.17. Similarly, 2.16, 2.15, 2.13 are the threshold values for refractive indices of Cs_2ScTlI_6, Na_2ScTlI_6 and K_2ScTlI_6. For the discussion of peak value $n(\omega)$ values reach its maximum peak in visible region and it decrease in UV region. Li_2ScTll_6 has highest $n(\omega)$ value than others due to the moderately thinner band gap of Li_2ScTlI_6(n = 2.66), it establishes the uppermost $n(\omega)$ value than C_2ScTlI_6, Na_2ScTlI_6, and K_2ScTlI_6(n = 2.63, 2.64, and 2.61). These results are predicting the utilization of these materials for solar cell and PV technologies as these materials showing highest values in the visible region for refractive indices.

Similar to the imaginary portion $\varepsilon_2(\omega)$ of the dielectric function, extinction coefficient $k(\omega)$ Fig. 5d also starts from a specific threshold energy. This threshold value corresponds to the value of materials band gap. Extinction coefficient $k_{max}(\omega)$ are 0.96 at 3.47eV, 1.08 at 3.58eV, 1.08 at 3.59 eV and 1.00 at 3.53 eV for $Cs_2ScTlI_6, Li_2ScTlI_6, Na_2ScTlI_6$, and K_2ScTlI_6 compounds, respectively.

Incident frequency vs reflectivity $R(\omega)$ for X_2S_{cT1I} with $X = Cs, Li, Na$ and K, displayed in Fig. 6a. Reflectivity $R(\omega)$ is the measure of quantity of light which is bounce back after hitting the materials interface. Static values of R(ω) which resemble to zero-frequency limit for $Cs_2ScTlI_6, Li_2ScTlI_6, Na_2ScTlI_6$, and K_2 ScTlII $_6$ are 0.135, 0.136, 0.1330.130 respectively. Sharp peaks in this case lies in visible and near UV $(2-4eV)$ spectra.

The materials exhibit high absorption coefficients in visible and UV ranges as can be seen in Fig. 6b. Similar to the imaginary portion $\varepsilon_2(\omega)$ of the dielectric function, and the extinction coefficient $k(\omega)$ absorption coefficients also initiates at some certain value of threshold energy which corresponds to the materials band gap energy. In the visible region of spectra material absorption shows regular behavior as it continues from threshold and tends to increases in both of visible and UV region. Materials showing high absorption coefficient of $\alpha > 10^5$ cm^{-1} in both visible and UV region making them excellent candidates for photovoltaic point of view.

All structures exhibit high optical conductivities in the region from 2-9 eV represented in Fig. 6c. High optical conductivity is shown by the material Cs_2ScTlI_6 of about 3.12fs^{-1} at 8.41 eV followed by K_2ScTlI_6 of valued 2.87fs^{-1} at 6.25 eV , and by Na_2ScTlI_6 of valued 2.83fs^{-1} at 7.81 eV , and by Li_2ScTlI_6 of valued 2.4fs^{-1} at 4.96 eV .

The electron energy loss (EEL) function of X_2ScTlI_6 with (X = Cs, Li, Na and K) in provided energy range of $0-9$eV presented in Fig. 6d. Sharp peaks in the energy loss function is closely related to the plasma oscillations which are known to be coincide with base of Re(ε) crossing the $x = 0$ line. The EEL function showing only one major peak at around 06 eV which is coinciding with plasma oscillations.

D. Mechanical Properties

Elastic constants are calculated in order to further calculate the materials mechanical parameters including value of different modulus like bulk modulus (B), shear modulus (G), and Youngs modulus (Y). From these values we further investigate the B/G ratio known as Pugh's ratio and v as Poisson's ratio which tells us about materials brittle and ductility. The critical value is near around 1.75[26] for the Pugh's ratio, below 1.75, material shows brittle nature, above 1.75 , it's ductile. The critical value for Poisson's ratio is about 0.26 , below this the materials is ductile and above this the material is ductile. Our results presented in the Table I showing the materials under consideration are of the ductile nature.

IV. CONCLUSION

A GGA-PBE study based on the pseudopotential under the framework of CASTEP was successfully done to obtained the structural, electronic and optical properties along with mechanical properties which are calculated under the frame work of Forcite module, of the X_2ScTlI_6 with (X = Cs, Li, Na and K) materials. The obtained direct band gap (2.05 eV to 2.42 eV) describes the semiconductor nature of these materials. High values of absorption coefficient (10^4 cm^{-1} to 10^5 cm^{-1}), refractive index (2.6-2.7), and real dielectric (06 to 08) along with low values of loss function ($0.25-0.50$), and reflectivity (0.20 0.25) all lies in the visible to UV-region $(03-06eV)$ of incident light indicating that the materials $X_2ScTl_1I_6$ with (X = Cs, Li, Na and K) can be

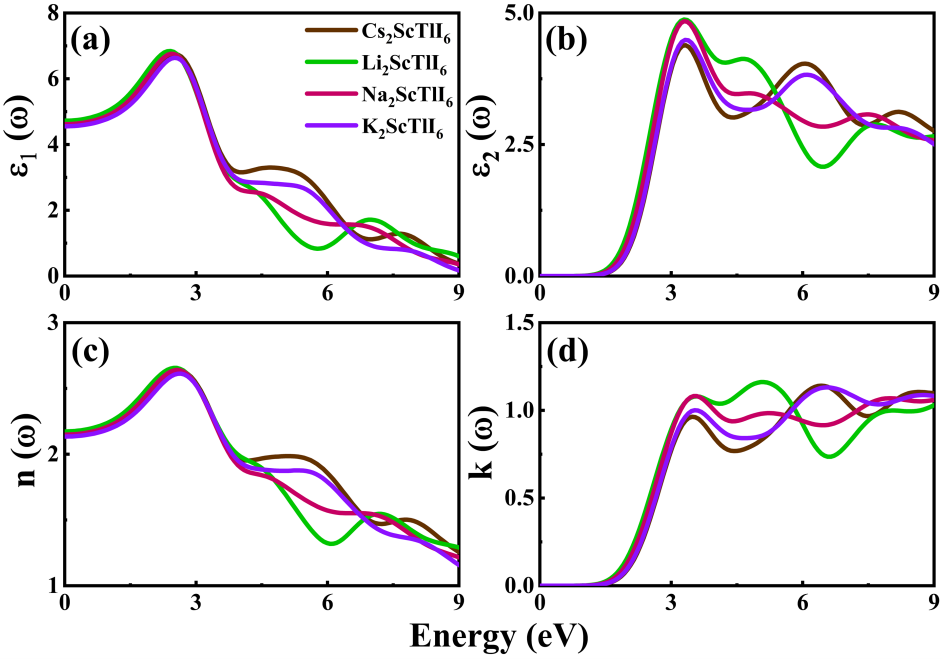

FIG. 5: Optical properties of materials (a) Dielectric function (real), (b) Dielectric function (imaginary), (c) Refractive index, (d) Extinction coefficient for X_2ScTlI_6 with ($X = Cs, Li, Na$ and K).

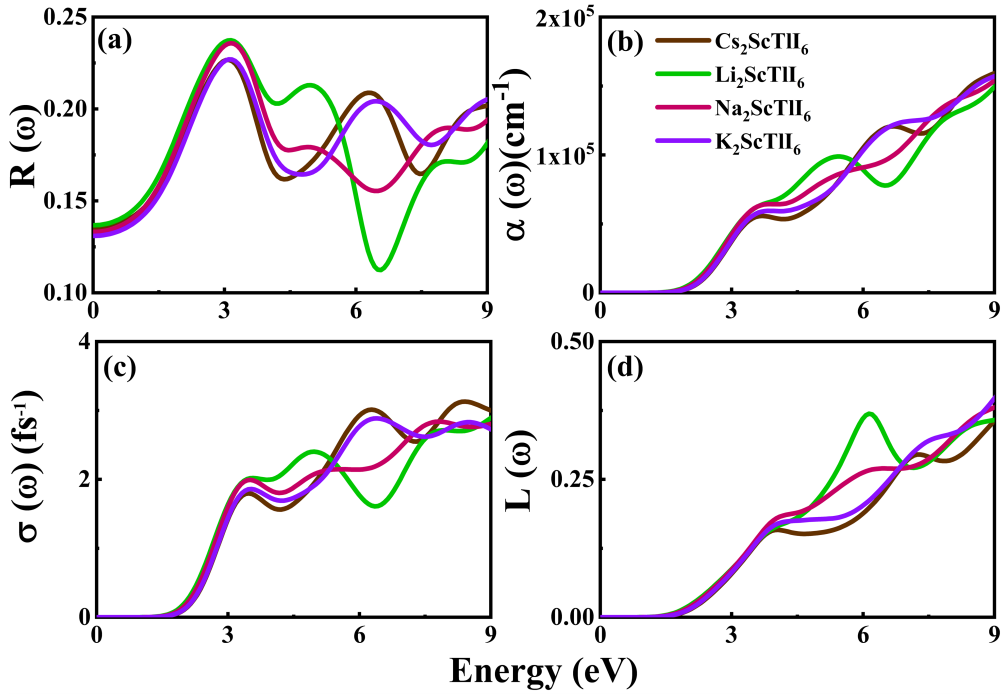

FIG. 6: Optical properties of materials (a) Reflectivity, (b) Absorption (c) Optical conductivity, (d) Loss function for $X_2ScTlI6$ with ($X = Cs, Li, Na$ and K).

TABLE I: values of elastic constant C_{ij} necessary for cubic symmetry, bulk modulus (B), shear modulus (G), Young's modulus (Y), Pugh ratio (B/G), for Poisson's ratio (v) of $X_2ScTlI6$ with ($X = Cs, Li, Na$ and K).

NAME	$Cs2_2ScTlI_6$	$Li_2ScTl\|_6$	Na_2ScTlI_6	K_2ScTll^6
C_{11}	5.5	1.6	1.8	3.6
C_{12}	4.2	1.0	1.5	2.1
C_{44}	1.3	0.5	0.3	1.0
B	4.7	1.3	1.8	2.7
G	0.5	0.3	0.3	0.7
Y	1.5	0.8	0.9	1.9
B/G	9.4	4.3	6.0	3.9
v	0.5	0.4	0.4	0.4

TABLE II: shows a comparison of some properties of our materials to those materials which previously predicted for Solar energy conversion.

Materials	Functional	Band Gap (eV)	Nature of band structure	Real dielectric function	Refractive index	B (GPa)	G (GPa)	Y (GPa)	References
Cs_2ScTII_6	GGA-PBE	2.42	Direct	6.75	2.63	4.7	0.5	1.5	This work
Li_2ScTlI_6	GGA-PBE	2.05	Direct	6.84	2.66	1.3	0.3	0.8	This Work
Na_2ScTII_6	GGA-PBE	2.27	Direct	6.72	2.64	1.8	0.3	0.9	This Work
K_2ScTlI_6	GGA-PBE	2.38	Direct	6.63	2.61	2.7	0.7	1.9	This Work
Cs_2AuYCl_6	GGA-PBE	2.05	Indirect	2.93	1.81	32.10	Gap	Gap	[13]
Cs_2AuYBr_6	GGA-PBE	1.56	Indirect	4.01	2.06	27.35	Gap	Gap	[13]
Cs_2AuYI_6	GGA-PBE	1.05	Indirect	5.87	2.45	22.19	Gap	Gap	[13]
$Na_2CuSbCl_6$	GGA-PBE	0.83	Indirect	4.48	2.13	10.29	5.81	15.98	[12]
$Na_2CuSbBr_6$	GGA-PBE	0.60	Indirect	4.99	2.25	8.44	8.65	20.18	[12]

used as potential applicant for the solar energy conversion devices. Moreover, mechanical properties including Pugh's ratio and Poisson's ratio indicating the ductile behavior of these materials.

DECLARATION OF COMPETING INTEREST

The authors have no conflicts to disclose.

ACKNOWLEDGMENT

Authors are thankful to the University of Lahore, Pakistan for the ORIC-SRGP 17/2024 research fund to support this research work. We are also pleased to acknowledge "1st International Conference on Sciences for Future Trends (ICSFT)- University of Lahore, Sargodha campus", for providing a valuable platform for sharing this research.

REFERENCES

[1] A. Hussain, F. Kainat, A. Hamza, A. Naz, N. Jabeen, T. Munawar, and M. A. Qaiser, "A dft study on the structural, electronic, optical, and elastic properties of blsfs xti$_4$bi$_4$o$_{15}$ (x = sr, ba, be, mg) for solar energy applications," Ceramics **7**, 1727–1741 (2024).

[2] L. Hernández-Callejo, S. Gallardo-Saavedra, and V. Alonso-Gómez, "A review of photovoltaic systems: Design, operation and maintenance," Solar Energy **188**, 426–440 (2019).

[3] A. Chaves, P. A. D. Gonçalves, and N. M. R. Peres, "Bandgap engineering of two-dimensional semiconductor materials," npj 2D Materials and Applications **4**, 29 (2020).

[4] M. Liu, M. B. Johnston, and H. J. Snaith, "Efficient planar heterojunction perovskite solar cells by vapour deposition," Nature **501**, 395–398 (2013).

[5] D. E. Carlson and C. R. Wronski, "Amorphous silicon solar cell," Applied Physics Letters **28**, 671–673 (1976).

[6] M. G. Panthani, V. Akhavan, B. Goodfellow, J. P. Schmidtke, L. Dunn, A. Dodabalapur, P. F. Barbara, and B. A. Korgel, "Synthesis of cuins$_2$, cuinse$_2$, and cu(in$_x$ga$_{1-x}$)se$_2$ (cigs) nanocrystal "inks" for printable photovoltaics," Journal of the American Chemical Society **130**, 16770–16777 (2008).

[7] K. W. Boeer, "p-type emitters covered with a thin cds layer show a substantial improvement of voc and ff," Solar Energy Materials and Solar Cells **95**, 786–790 (2011).

[8] C. W. Tang, "Two-layer organic photovoltaic cell," Applied Physics Letters **48**, 183–185 (1986).

[9] U.-G. Jong, C.-J. Yu, and Y.-H. Kye, "Computational prediction of structural, electronic, and optical properties and phase stability of double perovskites k$_2$snx$_6$ (x = i, br, cl)," RSC Advances **10**, 201–209 (2020).

[10]Q. Mahmood, M. Sohail, M. Imran, M. Usman, M. Usman, M. Usman, and M. Usman, "Optoelectronic and thermoelectric properties of double perovskite rb_2ptx_6 (x = cl, br) for energy harvesting: first-principles investigations," Journal of Physics and Chemistry of Solids **148**, 109665 (2021).

[11]H. Albalawi *et al.*, "Study of optical and thermoelectric properties of double perovskites cs2ktlx6 (x= cl, br, i) for solar cell and energy harvesting," Materials Today Communications **32**, 104083 (2022).

[12]A. Ayyaz *et al.*, "Structural, elastic, optoelectronic, and transport properties of na-based halide double perovskites na2cumx6 (m= sb, bi, and x= cl, br) as renewable energy materials: A dft insight," Journal of Materials Research **38**, 4609–4624 (2023).

[13]S. Mahmud, M. A. Ali, M. M. Hossain, and M. M. Uddin, "Dft mediated x2auyz6 (x= cs, rb; z= cl, br, i) double perovskites for photovoltaic and wasted heat management device applications," arXiv preprint arXiv:2404.15693 (2024).

[14]S. J. Clark, M. D. Segall, C. J. Pickard, P. J. Hasnip, M. J. Probert, K. Refson, and M. C. Payne, "First principles methods using castep," Zeitschrift für Kristallographie **220**, 567–570 (2005).

[15]J. P. Perdew, K. Burke, and M. Ernzerhof, "Generalized gradient approximation made simple," Physical Review Letters **77**, 3865–3868 (1996).

[16]P. Haas, F. Tran, P. Blaha, K. Schwarz, and R. Laskowski, "Insight into the performance of gga functionals for solid-state calculations," Physical Review B **80**, 195109 (2009).

[17]I. G. G. Apurba *et al.*, "Exploring the inorganic perovskite materials mg3sbx3 (where, x= i, br, cl and f) through the perspective of density functional theory: Adjustment of physical characteristics as consequence of strain," Heliyon **10** (2024), 10.1016/j.heliyon.2024.10.1234.

[18]N. Erum, J. Ahmad, M. A. Iqbal, and M. Ramzan, "Dft insights of mechanical, optoelectronic and thermoelectric properties for cs2sctlx6 (x= cl, br, i) double perovskites," Optical and Quantum Electronics **55**, 337 (2023).

[19]M. D. Segall, R. Shah, C. J. Pickard, and M. C. Payne, "Population analysis of plane-wave electronic structure calculations of bulk materials," Physical Review B **54**, 16317–16320 (1996).

[20]H. J. Monkhorst and J. D. Pack, "Special points for brillouin-zone integrations," Physical Review B **13**, 5188–5192 (1976).

[21]F. Kainat, N. Jabeen, A. Yaqoob, N. U. Hassan, A. Hussain, and M. E. Khalifa, "Effect of ca, ba, be, mg, and sr substitution on electronic and optical properties of xnb2bi2o9 for energy conversion application using generalized gradient approximation–perdew–burke–ernzerhof," Crystals **14**, 710 (2024).

[22]M. A. Momin, M. A. Islam, M. Nesa, M. Sharmin, M. J. Rahman, and A. H. Bhuiyan, "Effect of m (ni, cu, zn) doping on the structural, electronic, optical, and thermal properties of cdi2: Dft based theoretical studies," AIP Advances **11**, 055203 (2021).

[23]A. Hussain, F. Kainat, N. Jabeen, A. Yaqoob, T. Abbas, M. U. Khan, M. A. Qaiser, and M. H. H. Mahmoud, "First-principles calculations of the structural, mechanical, optical, and electronic properties of x2i4i5o18 (x = pb, ba, ca, and sr) bismuth-layered materials for photovoltaic applications," Crystals **14**, 870 (2024).

[24]Z. Abbas, M. A. Islam, M. A. Momin, M. Sharmin, M. J. Rahman, and A. H. Bhuiyan, "Effect of nb, ta and v replacements on electronic, optical and elastic properties of nbcu34 a gga+u study," Journal of Solid State Chemistry **301**, 122338 (2021).

[25]R. Hill, "The elastic behaviour of a crystalline aggregate," Proceedings of the Physical Society. Section A **65**, 349 (1952).

[26]S. F. Pugh, "Xcii. relations between the elastic moduli and the plastic properties of polycrystalline pure metals," The London, Edinburgh, and Dublin Philosophical Magazine and Journal of Science **45**, 823–843 (1954).

[27]M. Hussain, A. Hussain, M. A. Momin, M. A. Islam, M. Sharmin, M. J. Rahman, and A. H. Bhuiyan, "Systematic study of optoelectronic and transport properties of cesium lead halide (cs2bx6 x = cl, br, i) double perovskites for solar cell applications," Ceramics International **46**, 21378–21387 (2020).